CHAPTER-6

RESULTS AND DISCUSSION: TiC PARTICULATE REINFORCED METAL MATRIX COMPOSITES

RESULTS AND DISCUSSION: TiC PARTICULATE REINFORCED METAL MATRIX COMPOSITES

The microstructures, mechanical and tribological properties of TiC particulates reinforced magnesium alloy composites have been investigated in this chapter. The effect of small variation (3, 6, 9 and 12 wt %) of reinforcements has been reported in this study. The results have been discussed to develop a coherent understanding of the phenomenon.

6.1. Introduction

Particulate reinforced metal matrix composite is easily manufactured under controlled atmosphere through the stir casting process. TiC particulates possess many desirable properties, such as low density, high hardness, high modulus, and high wear resistance.

The effect of small variation (3 %, 6 %, 9 % and 12 % by weight) of TiC particles (average size 20 μm) is used to develop AZ91 magnesium alloy based metal matrix composites in the current study. The vacuum assisted stir casting process is used for the synthesis of composites. The variation in density with the addition of different (3, 6, 9 and 12) wt % of TiC in AZ91 magnesium alloy is presented and discussed in this Chapter. The microstructural features and X-ray diffraction analysis is conducted to revealed different phases present in the AZ91 alloy and its composites. All the characterizations, testings and wear behaviors which are used in Chapter 5 for SiC particulates reinforced composites are also performed on the composites reinforced by the different percentage of TiC particulates.

6.2. Results and discussion

6.2.1. Density Measurement

Table 6.1 gives the results of density measurements of monolithic AZ91 and its composites. The measured densities of the composites are very close to that of the theoretical values. Thus, near-dense and approximately porosity free composites can be consistently produced using the vacuum-assisted stir casting methodology, which is adopted in the current study. However, as the amount of reinforcement increases the porosity is slightly increased.

Table 6. 1: Density and porosity measurements of AZ91 alloy and its composite reinforced with TiC particulates

Materials	**Reinforcements (Wt %)**	**Theoretical Density (g/cm^2)**	**Experimental Density (g/cm^2)**	**Porosity (%)**
AZ91	0	1.8101	1.8005	0.53
AZ91+3 % TiC	3	1.8451	1.8201	1.35
AZ91+6 % TiC	6	1.8815	1.84865	1.74
AZ91+9 % TiC	9	1.9194	1.87745	2.18
AZ91+12 % TiC	12	1.9588	1.9109	2.44

The density values of the composites are in general higher than the monolithic alloy of magnesium. Further, the density value is found to increase with the increasing weight percentage of TiC particulate, and it is due to the presence of comparatively higher density TiC particulate in magnesium alloy [208], [222]. The porosity also exhibits a gradual increase as the weight percentage of reinforcement's increases in the composite. The increase in porosity in composites is due to increase in micro-voids near the vicinity of the large TiC particle. Similar observations are also reported by other authors [130], [223] about magnesium alloy based metal matrix composites.

6.2.2. Microstructure Characterization

Microstructural characterization studies are carried out by optical microscopy (OM) and scanning electron microscope (SEM) [209] TiC particulates reinforced AZ91 magnesium alloy composites, in order to examine the morphological characteristics of grains, presence of porosity, distribution of TiC particulates, and interfacial characteristics of TiC particulates with the AZ91 magnesium alloy matrix [210]. The sample for the microstructural characterization was prepared by cutting, grinding and polishing on different grit size of the abrasive paper. Microstructural characterization was carried out on the etched AZ91/TiC composites samples using a Leica optical microscope (OM) equipped with Leica application suite and ZEISS scanning electron microscopes (SEM) equipped with energy dispersive spectroscopy (EDS). Homogeneous distribution of reinforcements should be achievable irrespective of the size and amount of the reinforcements. However, at a higher percentage of TiC particulate, some clustering is observed in the fabricated composites. The optical microstructure of AZ91 with a different percentage of TiC particle reinforced composite has been illustrated in Figure 6.1. In this Figure, the β- phases are represented by red arrows, α- phases are represented by the blue arrow, the reinforcements are represented by a black arrow, and the porosities are represented by the yellow arrow. The increase in the percentage of the TiC particle leads to a decrease in the grain size of the magnesium alloy. It is clear that the addition of TiC reinforcement in AZ91 magnesium alloy is responsible for the refinement of grain size in the stir cast composite. The β-phases are generally having the composition of $Mg_{17}(Al, Zn)_{12}$. The red arrows represent the grain boundary in AZ91 alloy. Figure 6.2 shows the optical micrograph of the TiC/AZ91 magnesium alloy composite at higher magnifications. The reinforced particles are observable in the microstructure.

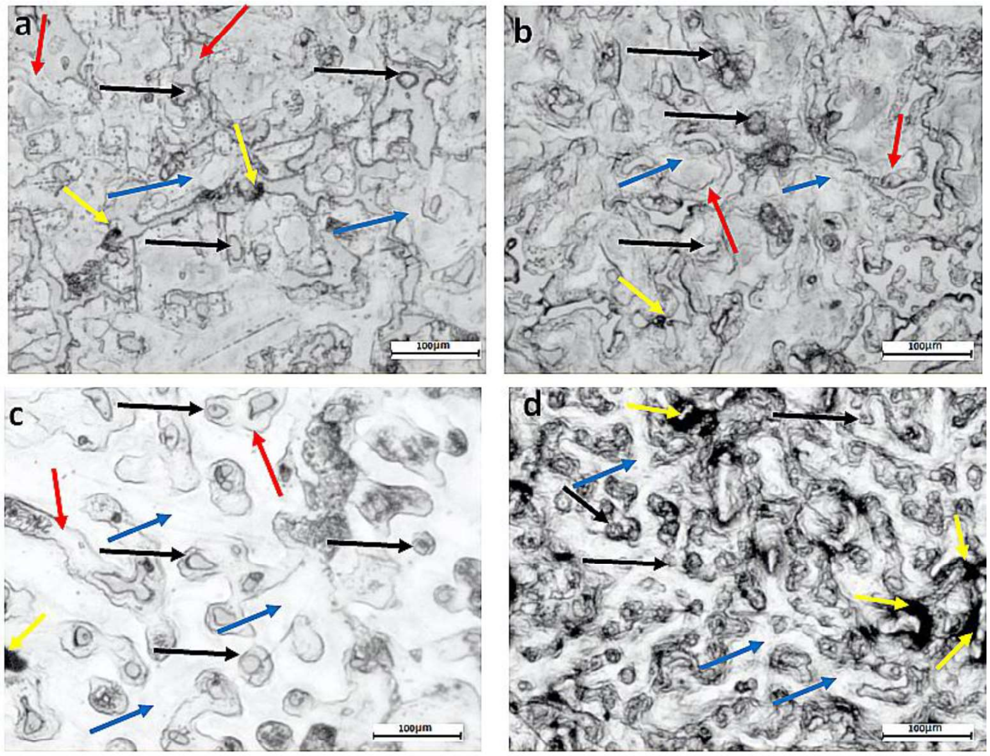

Figure 6. 1: Optical micrograph of TiC/AZ91 magnesium alloy composite at different weight percentage a) 3 % TiC b) 6% SiC c) 9% TiC d) 12 % TiC

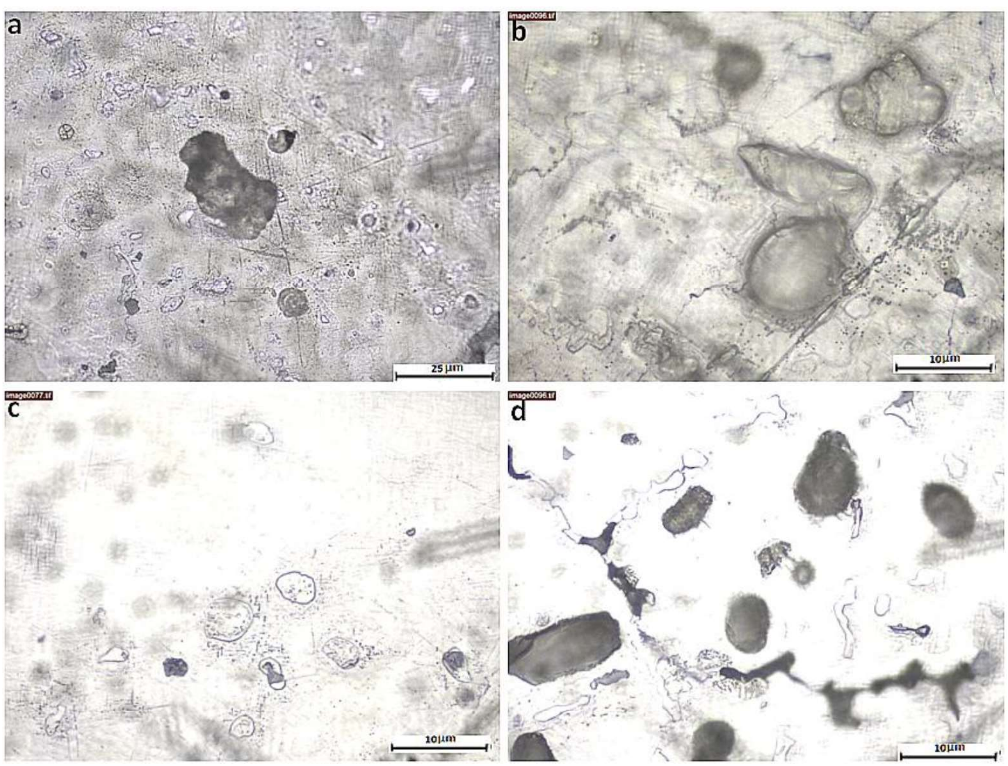

Figure 6. 2: Optical Micrograph of TiC/AZ91 magnesium alloy composite at higher magnifications a) 3 % TiC b) 6% TiC c) 9% TiC d) 12 % TiC

The bright area in magnesium alloy morphology is found to be dendritic. The grains are refined in the addition of TiC particulate in AZ91 magnesium alloy. The reduction in grain size may be attributed due to enhanced nucleation effect offered by TiC particulates. The hard reinforced particle seems to be embedded in the matrix of the composites. The wettability of the reinforcement is assumed to be good as a reinforced particle are tightly bonded with the matrix materials. The shape and size of the particle are not uniform, so there is the possibility of the small void/ cavity in the vicinity of the reinforcement due to the addition of discontinuous reinforcement, which results in porosity in the composites.

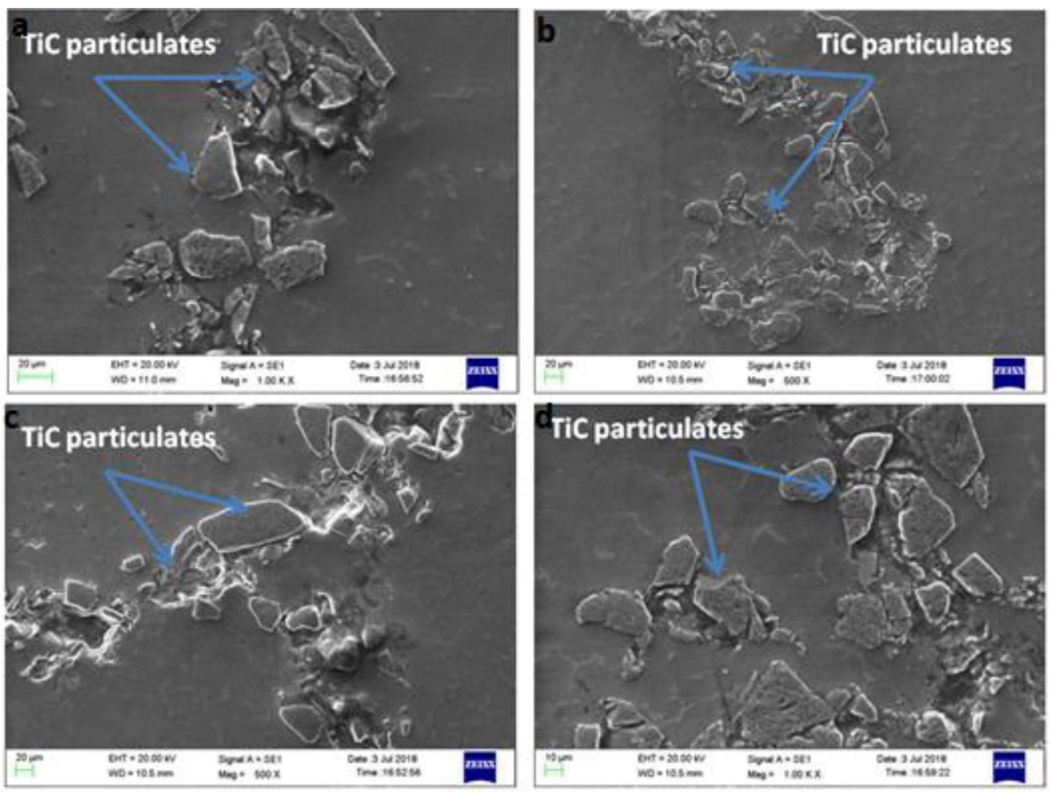

Figure 6. 3: SEM micrograph showing distribution of TiC particulate in AZ91 magnesium alloy (a) 3 % TiC (b) 6% TiC (c) 9% TiC (d) 12% TiC

Figure 6.3 shows the FEM micrograph of TiC particulate reinforced composites at a different percentage of TiC particulates. The distribution of TiC particulates in AZ91 magnesium alloy is fairly uniform, but in some places, the accumulation of particles is seen. Blue arrows mark the TiC particulate reinforcement.

6.2.3. X-Ray diffraction

Figures 6.4 show the X-ray diffraction pattern corresponding to magnesium alloy AZ91 and its composites with 3, 6, 9, and 12 weight % of TiC particulates. The lattice spacing's (d) obtained were compared with that of pure magnesium, TiC_p, and $Mg_{17}Al_{12}$ which is available in JCPDS/PCPDFwin data. The XRD analysis for phase identification revealed the presence of the magnesium matrix, the inherent inter-metallic phase $Mg_{17}Al_{12}$. However, the peaks of TiC is not clear because the highest intensity peaks of TiC is below 400 counts (which is negligible in comparison to several thousands of AZ91). A comparative plot of peaks of TiC particulates and AZ91alloy are shown in Figure 6.5. All the peaks are leveled according to their presence in the intensity plot of the XRD data. The results, in particular, show the absence of MgO due to presence vacuum and argon gas inert atmosphere during.

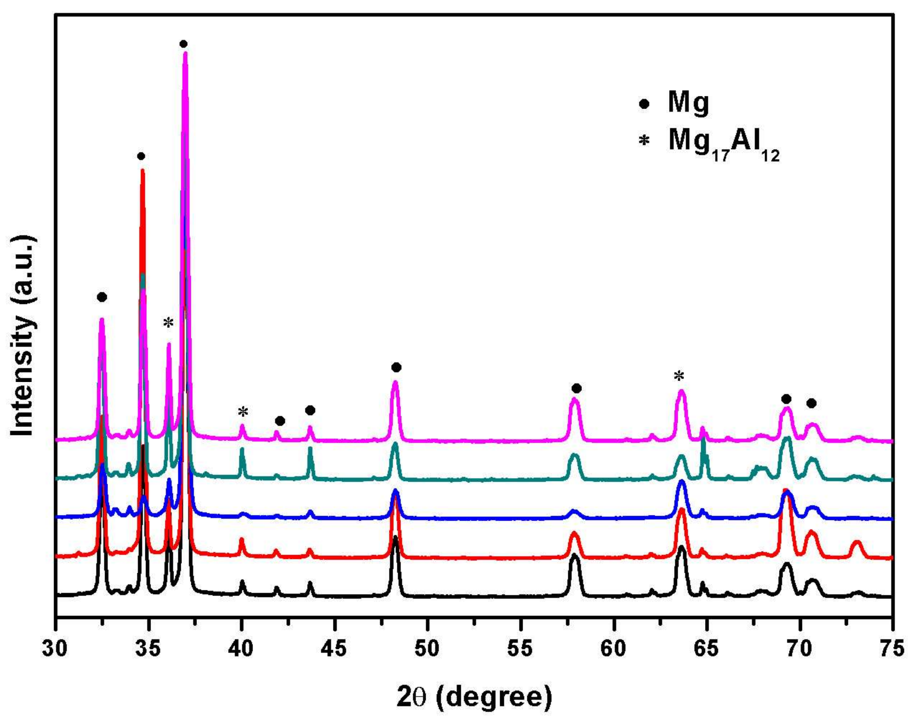

Figure 6. 4: X-ray diffraction analysis of magnesium alloy and its composites with different (3%, 6%,9%, and 12%) weight percentage of TiC particulates

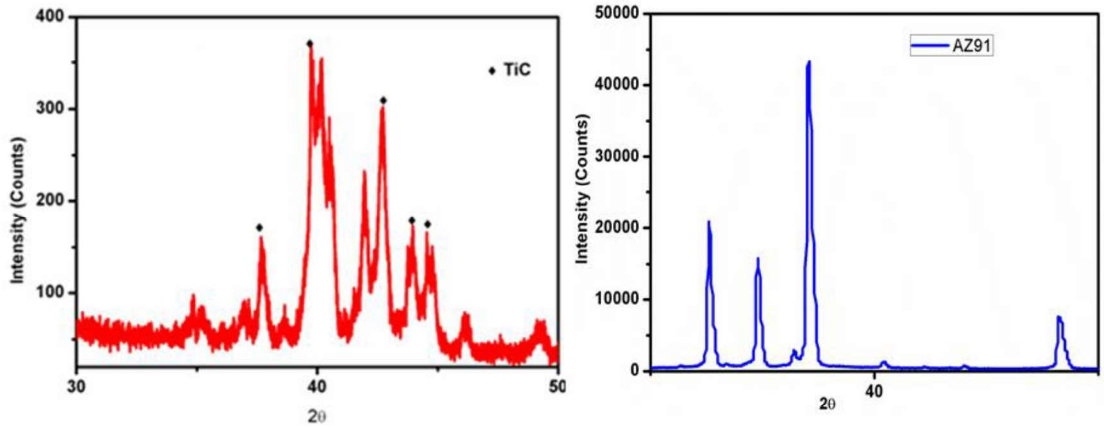

Figure 6. 5: Comparative plot of peaks of TiC particulates and AZ91 magnesium alloy

6.2.4. Hardness Test

Vickers microhardness is investigated to know the homogeneous distribution of TiC particles within magnesium alloy (AZ91). A rectangular cross-section sample (15 mm x 30 mm) of each fabricated composite has been used to measure the Vickers hardness. The Vickers microhardness value examined throughout the cross-section at ten different points of the AZ91 alloy and its composites reinforced with TiC particulates. There was slight variation in hardness value at different point of the cross-section of the AZ91 alloy and its composites; it shows a relatively uniform distribution of TiC particle within a magnesium alloy matrix. The variation in hardness in AZ91 alloy is due to the presence of hard intermetallic secondary phase of magnesium alloy in reaction with aluminum. The variation in composites is due to the presence of different size of reinforcement as well as slight accumulation of particle at some places. Figure 6.6 shows the variation in microhardness value of magnesium alloy (AZ91) and its composites reinforced with TiC particle with a weight percentage variation of 3%, 6%, 9%, and 12%. From Figure 6.6 it is observed that there is a random variation in hardness with an increase in the hardness when the content of reinforcement is increased from 3 to 12 weight percent at ten different points of the sample. The average

Vickers micro hardness of the magnesium alloy AZ91 and its composites reinforced with TiC particulate are shown in Table 6.2 and Figure 6.7. The hardness value of the composite is increased as the percentage of TiC reinforcement increases. The Vickers hardness value is increased by ~25% on addition of 3% of TiC particulate, and it further increased up to ~75% on addition of 12 % of TiC particulate.

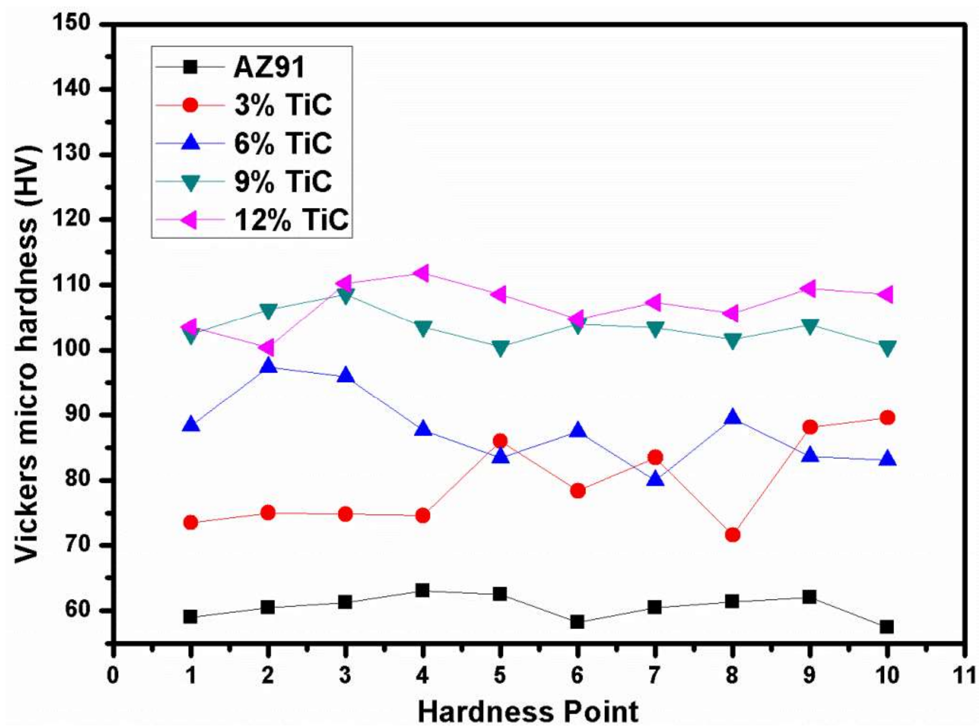

Figure 6. 6: Variation of Vickers microhardness of magnesium alloy and its composites reinforced

The observed hardness value of the composites with different percentage of TiC (3 %, 6 %, 9 % and 12%) particulate are found to be higher than magnesium alloy because of the interactive influence of the presence of TiC particulates and finer grain size of the composites, which restrict the localized matrix deformation during indentation. The presence of hard TiC particles will increase the load bearing capacity and also restrict the deformation of the matrix by constraining the dislocation movement. The hardness value of the magnesium alloy composites increases with the increase in the weight percentage TiC particulate reinforcement.

Table 6. 2: The average Vickers microhardness of magnesium alloy and its composite

Sr. No	Materials	Hardness
1.	AZ91	60 ± 1.8
2.	AZ91+3%TC	74.65±3
3.	AZ91+6%TiC	93.25±2.5
4.	AZ91+9%TiC	102±4
5.	AZ91+12%TiC	105±3.4

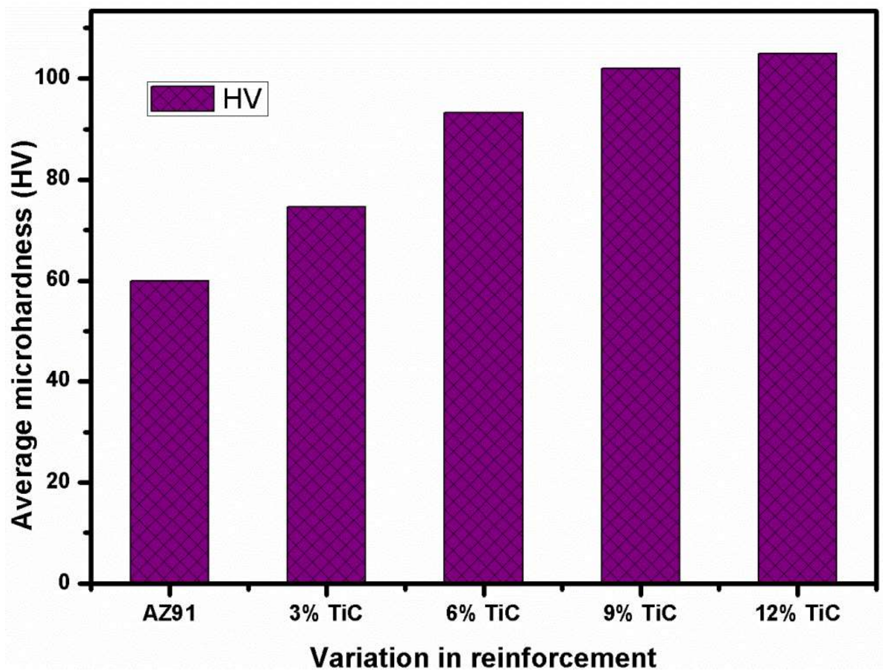

Figure 6. 7: Average Vickers microhardness of AZ91 alloy and its composite with different percentage of TiC particulates reinforcement

6.2.5. Tensile Test

The ultimate tensile strength and yield strength of the AZ91 and its composite with different wt % of TiC (3, 6, 9 and 12) are given in Table 6.3. Figure 6.8 shows the engineering stress-strain curve of magnesium alloy AZ91 and its composite reinforced with a different weight percentage of TiC particulates under tensile loading. The graphical bar charts representation of the yield strength and ultimate tensile strength are presented in Figure 6.9. The ultimate tensile strength (UTS) of magnesium alloy (AZ91) is found to be ~188 MPa. The ultimate tensile strength of the 3% TiC particulate reinforced composite is lower than that of the magnesium alloy, and it increases with increasing the wt % of reinforcements. However, the ultimate tensile strength of 12% TiC particulate reinforced composite is ~194 MPa, which is higher than that of magnesium alloy AZ91. For the as-cast AZ91 composite ultimate tensile strength usually lower than that of as-cast AZ91 [211] because of the addition of any secondary hard phase particle reduces tensile strength in the as-cast state.

Further secondary processing such as extrusion, forging and rolling operation may have enhanced properties due to the formation of the strong bond between reinforcement as well as the absence of microvoids and porosity in as-cast composites. The yield strength of the composites is observed to be increasing with the increase in weight percentage of TiC particles in magnesium alloy (AZ91) composites as depicted in Table 6.3 and Figure 6.9. The various strengthening mechanism can contribute to increased yield strength of the metal matrix composite, i.e. (a) Generation of geometrically necessary dislocation to accommodate thermal and elastic modulus mismatch between the matrix and reinforcement (b) Load- bearing effects due to the presence of reinforcement (c) Orowan strengthening (d) Hall- Petch effect due to grain size refinement. The detail of different mechanism and mode of stress increment has already discussed in the literature review, i.e. Chapter 2

Table 6. 3: The ultimate tensile strength and yield strength

Materials	**UTS (MPa)**	**YS (MPa)**
AZ91	187.67	120.9
AZ91+3% TiC	167.1	128.9
AZ91+6% TiC	178.5	141
AZ91+9% TiC	198.2	148.8
AZ91+12% TiC	202	152

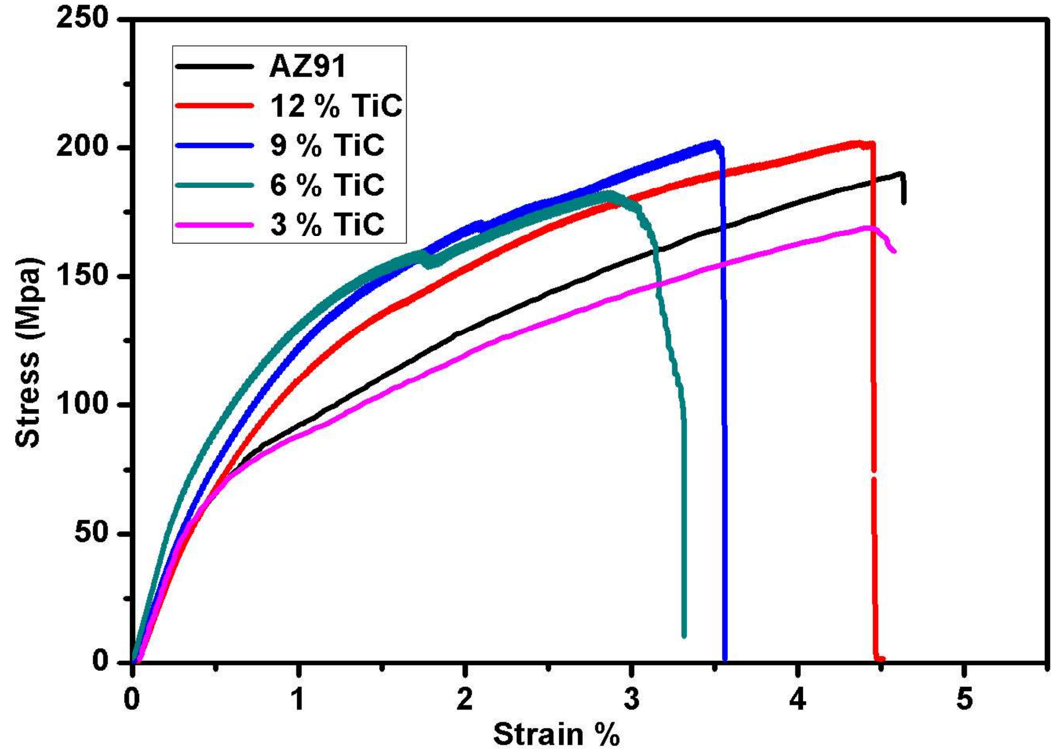

Figure 6. 8: Engineering stress-strain curve of AZ91 and its composite reinforced with TiC particulates

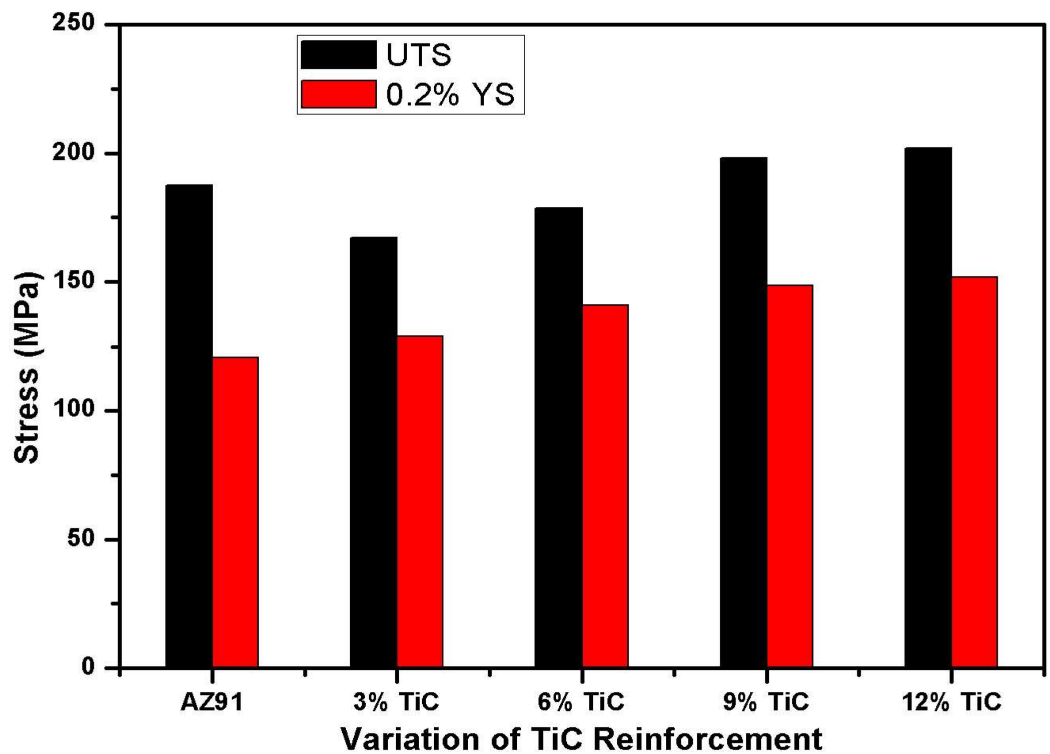

Figure 6. 9: Variation of ultimate tensile strength and yield strength with a variation of TiC particulates

6.2.6. Compressive test

The compression tests of AZ91 alloy and its composites have been performed, and the results are shown in Table 6.4. Figure 6.10 shows the graphical representation of the ultimate compressive strength in MPa. The ultimate compressive strength of the composite materials reinforced with TiC particulate is higher than unreinforced AZ91 magnesium alloy as depicted in Figure 6. 10. The ultimate compressive strength of the composite further increased as the weight percentage of TiC particulate increases in base alloy AZ91. The ultimate compressive strength of the composite increases because of the addition of hard particle in a softer matrix will increase load-bearing capacity, and effective load transfer is highly dependent upon the interfacial bonding between the matrix and the reinforcement. The significant improvement in ultimate compressive strength was observed in the TiC particulate reinforced composite in comparisons with monolithic alloys. The enhancement in ultimate compressive strength may be attributed due to the partial closure of the small microscopic cracks during compressive loading. A similar observation is also reported for SiC_p reinforced AZ92 magnesium alloy composites [212]. The Compressive strength is increased by ~2% on addition of 3% of TiC particulate, and it further increased up to 15 % on the addition of 12 % of TiC particulate.

Table 6. 4: Ultimate compressive strength of AZ91 alloy and its composites reinforced with different weight percent of TiC

Materials	**Ultimate Compressive Strength (MPa)**
AZ91	308
AZ91+3%TiC	313
AZ91+6%TiC	326
AZ91+9%TiC	337
AZ91+12%TiC	355

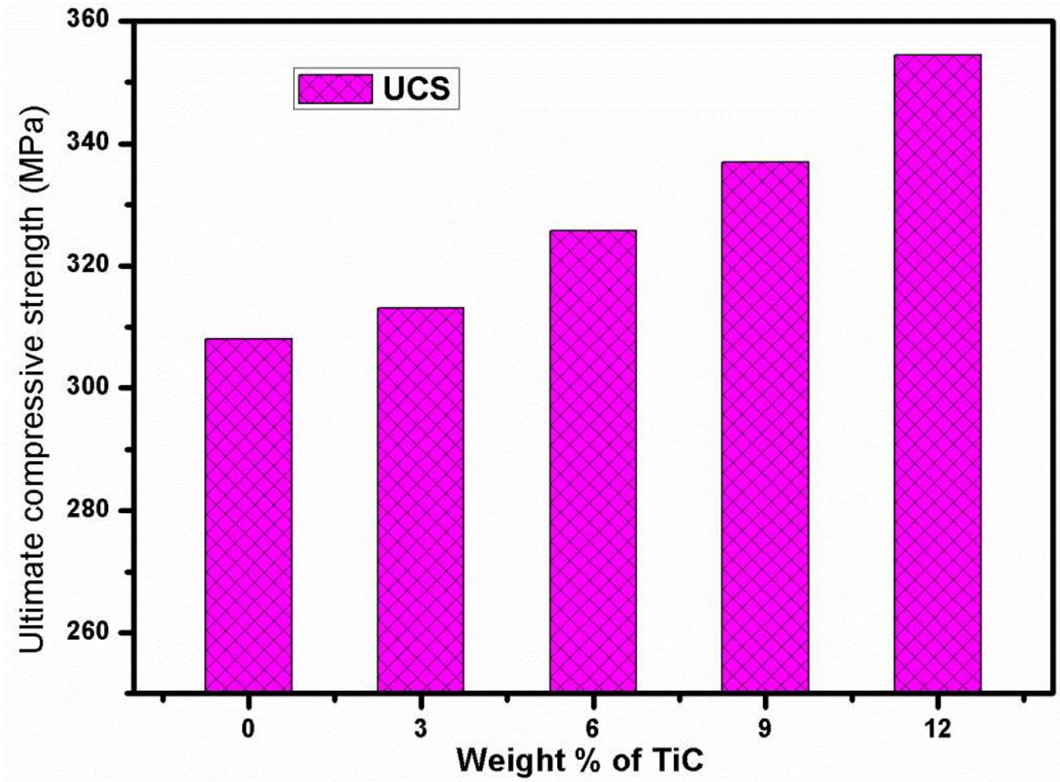

Figure 6. 10: Representation of the ultimate compressive strength of AZ91 alloy and its composites reinforced with different weight percentage of TiC

6.2.7. Factograph after tensile Test

The magnesium and its alloy at room temperature show dominant brittle fracture because of the HCP structure. The HCP structures have a limited number of a slip in its structures. The fracture surfaces of the magnesium alloy AZ91 and as-cast composites reinforced with different wt % (3, 6, 9 and 12) of TiC particulates are microscopically rough with a typical height variation of 2 mm. Figure 6.11 shows the SEM image of fracture surfaces of as-cast magnesium alloy AZ91 based composites reinforced with a different weight percentage of TiC particulates at different magnification. The main features of the fracture surface are locally concentrated TiC particles and agglomeration of TiC particles. De-bonding of the particle/matrix interface, cracks on the particles and inter-granular cracks in the matrix is also present.

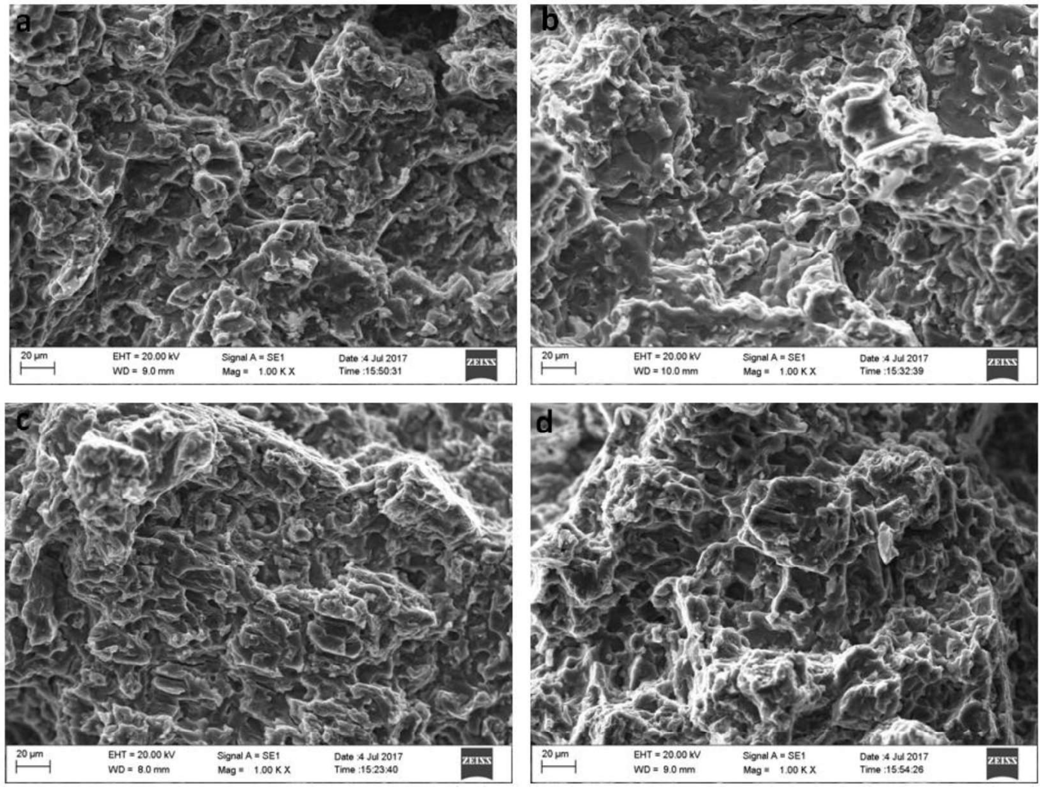

Figure 6. 11: SEM micrograph of cast magnesium alloy AZ91 based composites a) 3% TiC b) 6% TiC c) 9% TiC d) 12% TiC

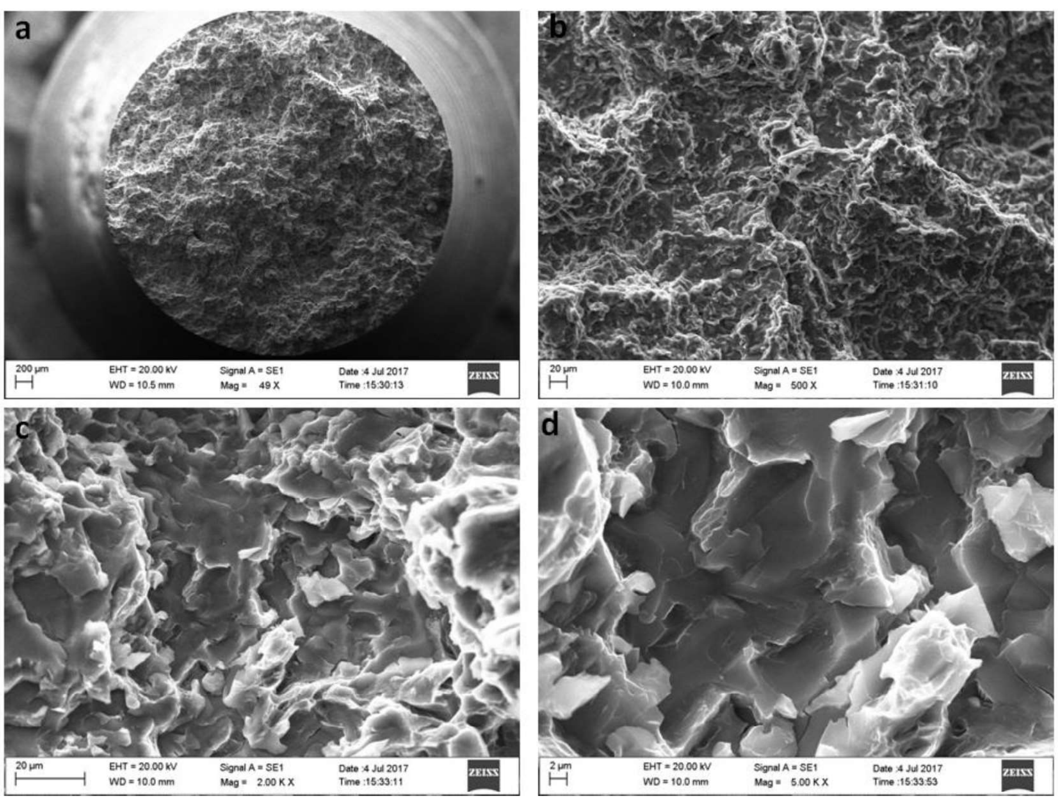

Figure 6. 12: SEM micrograph of 6 % TiC reinforced magnesium alloy composites at different magnification a) 49X b) 500X c) 2000X d) 5000X

Figure 6.12 shows the SEM micrograph of 6% TiC reinforced magnesium alloy composites at different magnifications. From the fracture surface investigation, it has been seen that the fracture occurred via two types in case of the composite. In the matrix phase, dominant regions are a ductile fracture of the matrix takes place in which void nucleation could play an important role. The brittle fracture occurs where the concentration of TiC particle is high. The composite tends to exhibit more brittle fracture morphology than the matrix alloy. The crack of the composite is started by de-bonding at the interface of the matrix and TiC reinforcement.

1. In the case of the matrix, the fracture occurs by cleavage mode, interspersed with the ductile feature.
2. The composite shows mixed mode fracture (i.e., ductile and cleavage), particle de-bonding is also observed.
3. The matrix particle interface would be predominantly governed by mechanical bonding, hence when the maximum load is reached rather than particle fracture de-bonding of TiC particles occurs.
4. The fracture surface morphology of the composite also reveals that small size dimple, micro-crack, and cleavage fracture increases with increase in reinforcement.

6.2.8. Pin on disk sliding wear test

Pin on disk dry sliding friction and wear testing machine is used to evaluate the tribological characteristics of the magnesium alloy and its composite with different percentage of TiC particulate. The wear sample is made as per ASTM standard: G99. The friction wear weight losses are generated by varying the normal load at two different velocities for all the composites. Fabricated AZ91 alloy based metal matrix composite materials in this work are supposed to offer some impending benefits for tribological applications where materials with lower density are required. The specimens are weighed before and after the test using a balance having an accuracy of 0.0001 gm to measure the weight loss. The wear rate is calculated from the volume loss divided by sliding distance. The data for the wear tests are taken from the average of the three measurements. The worn surfaces are observed using the scanning electron microscopy (SEM) and before that the worn surfaces are cleaned thoroughly to remove the loose wear debris.

a) Dry sliding wear test parameter and wear behavior

The dry sliding wear test for AZ91 alloy and its composite with the different percentage (3, 6 9 and 12) of TiC_p has been performed. The variations of sample weight loss with constant sliding speed are observed under variable normal load from 9.81 N (1 Kgf) to 58.86 N (6 Kgf). Different parameters used in dry sliding wear test are tabulated in Table 6.5. The formula used for calculation of sliding velocity (v) and sliding distance (l) are already given by equation (5.1) and (5.2) in Chapter 5:

Table 6. 5: Parameters for the pin on disk dry sliding wear test

Sr. No	Parameters	Value/ description
1.	**Pin materials**	AZ91 and its composite reinforced with TiC (3%, 6%, 9%, and 12%)
2.	**The dimension of the Pin**	30 mm length and 8 mm in diameter
3.	**Disk Material**	Tool steel grade EN31
4.	**Track diameter (D)**	83 mm for all experiments
5.	**Load Variation (N)**	9.81 N, 19.62 N, 29.43 N, 39.24 N, 49.05 N, 58.86 N (for RPM-320)
		19.62 N, 39.24 N, 58.86 N (for RPM-600)
6.	**Sliding Time (t)**	15 minutes
7.	**Speed Variation (n)**	320 RPM and 600 RPM

The wear weight loss of AZ91 alloys and TiC particulates reinforced composites are plotted against different normal loads at the constant sliding speed of 1.39 m/s in Figure 6.13. The wear weight loss of unreinforced magnesium alloy having a higher value than composites at all the normal load for sliding speed of 1.39 m/s as seen in Figure 6.13. As the percentage of reinforcement increases in the composite, the wear weight loss decreases for all the different (3, 6, 9 and 12) percentage of the TiC particulates reinforced composites. However weight loss for the composite increases with an increase in normal applied load. The estimation of wear weight or wear volume may be calculated by Archard's law [161].

The adhesive wear generally associated with low normal load and low sliding velocity. The others wear mechanism also involved in the material removal process of dry sliding wear. The combined effect different wear mechanism involved in the estimation of wear loss. The addition of hard particle (TiC) in base alloy AZ91 may provide dry lubrication, and it can provide rolling contact between the hard disk materials and soft pin materials. Therefore, on increasing amount of reinforcement the wear weight loss and wear volume decreases in the case of particulates reinforced composites. Figure 6.14 shows the wear rate (mm^3/m) at different normal load. It seems that wear rate is greater at the higher load and the wear rate decreased on increasing the weight percentage of TiC particulate reinforcement. The wear rate plot with respect to applied normal load is almost linear which is in conforming to the Archard's law. The variations of the average sliding coefficient of friction (μ) with a different value of applied normal loads are shown in Figure 6.15. The average coefficient of friction is decreased as the normal load increases in all the cases, irrespective of alloy and composite. The average coefficient of friction value at lower load is slightly different from its behaviors at higher loads. The unreinforced alloy has higher value of the coefficient of friction than TiC particulate reinforced composite. Figure 6.16 shows the average sliding coefficient of friction (μ) with different percentage of TiC particulate reinforcements. It is clear from Figure 6.16 that the coefficient of friction for alloy composite at lower load is higher than its value at higher. The small variation in coefficient of friction was observed in composites at higher load and a higher percentage of reinforcements. These behaviors can be explained with the phenomenon that on increasing applied normal load the asperities of the mating surfaces will be deformed, and this led to a decrease in coefficient of frictions. The coefficient of friction is almost constant at higher load. The wear rates at two different speeds with respect to three different loads are presented in Figure 6.17 to Figure 6.21 for the monolithic alloy, and it composites reinforced with different percentage of TiC particulates.

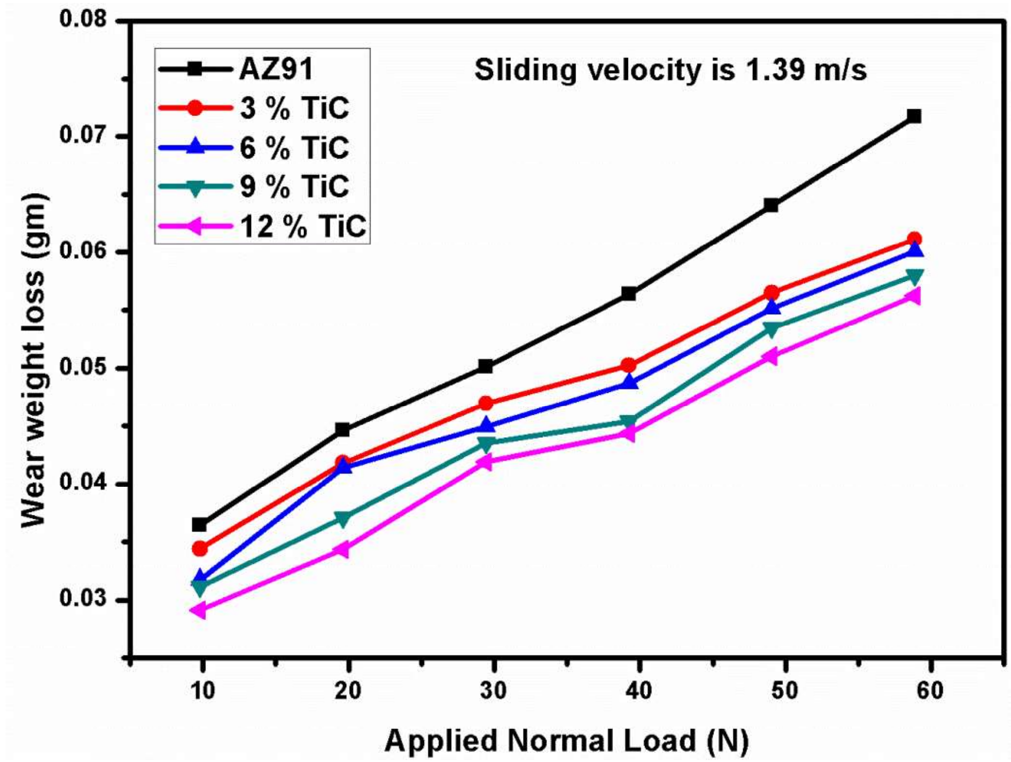

Figure 6. 13: The variation of wear weight loss with different normal load at sliding speed of 1.39 m/s

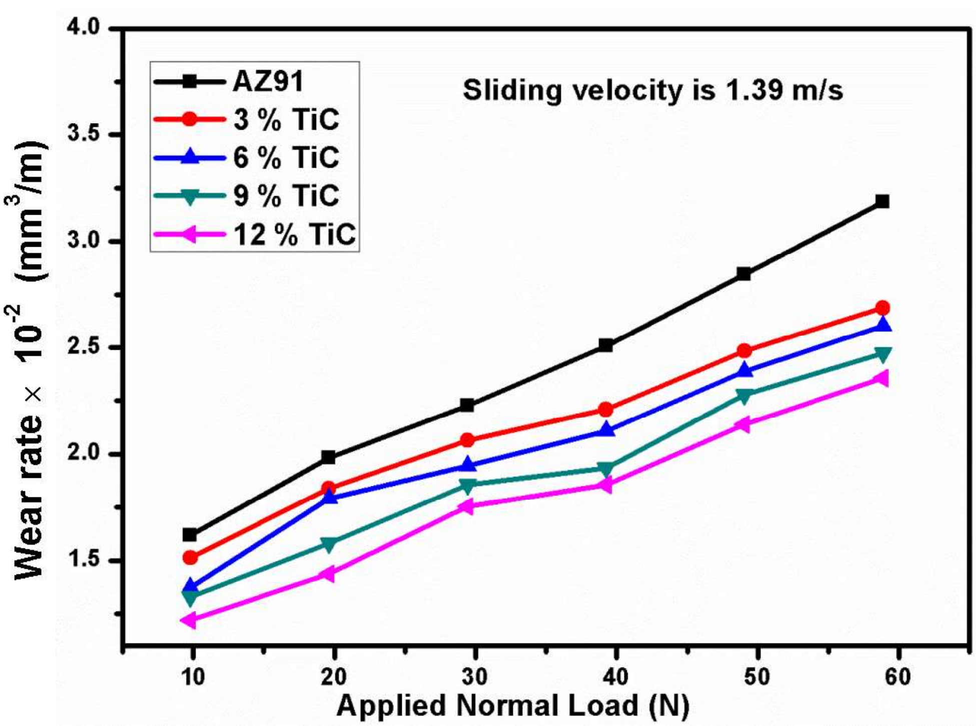

Figure 6. 14: The variation of wear rate with an applied normal load of AZ91 magnesium alloy and its composite reinforced by TiC particulates

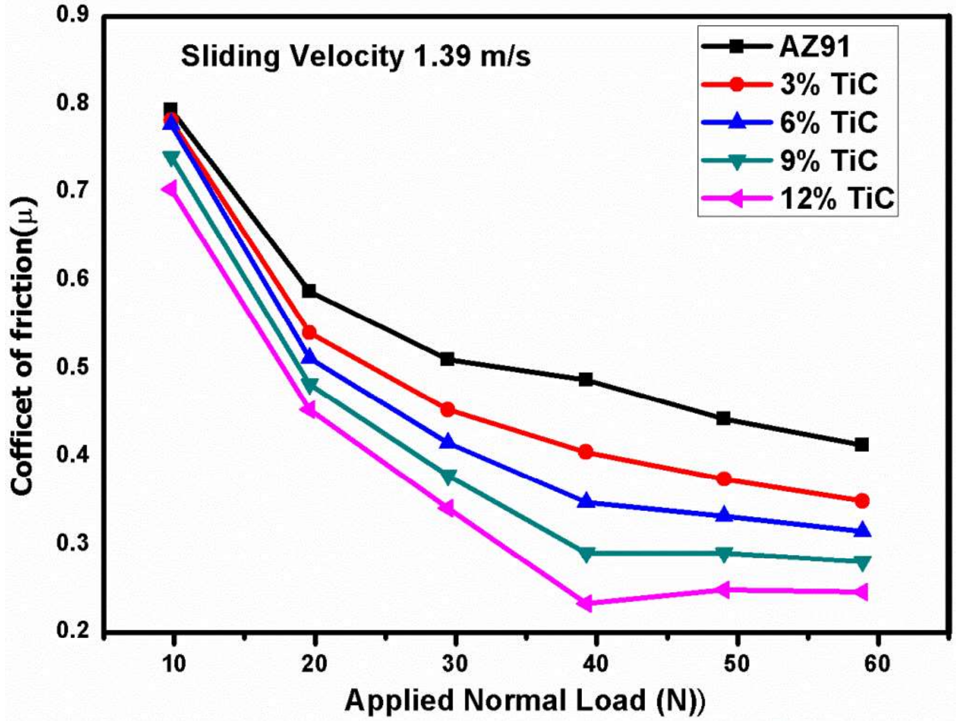

Figure 6. 15: Average coefficient of friction of the AZ91 magnesium alloy and its composites reinforced with TiC particulates at different applied normal load

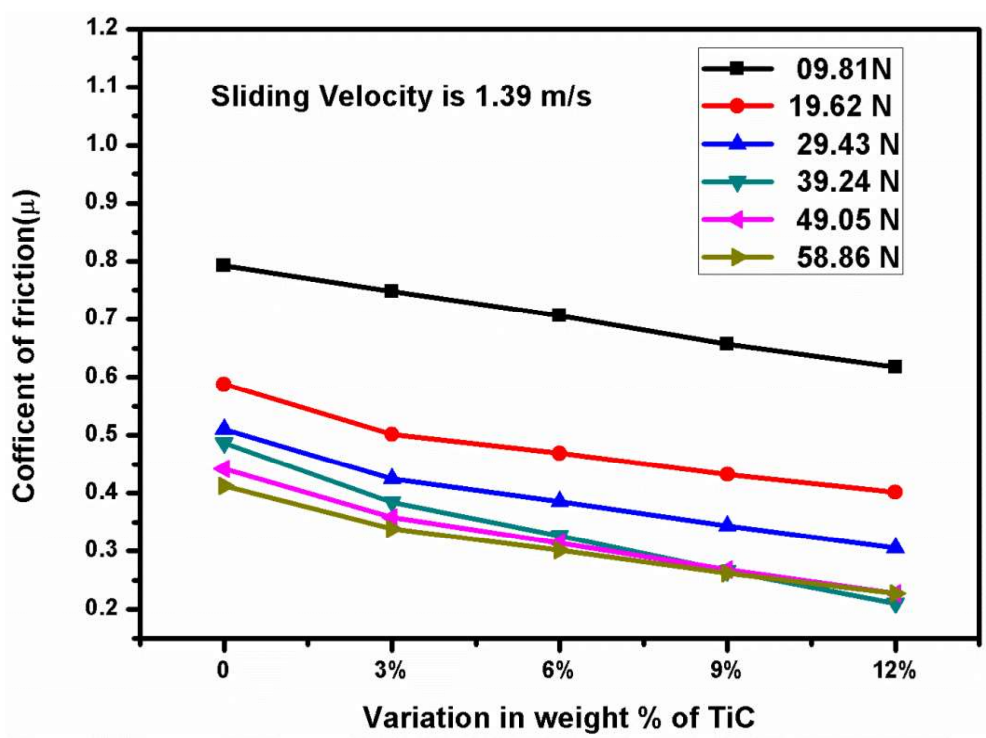

Figure 6. 16: Variation average coefficient of friction of the AZ91 magnesium alloy and its composites at a different weight percentage of TiC and different applied normal load

It can be seen from the Figures 6.16 to 6.21 that the wear rates at the sliding speed of 2.60 m/s are higher than the wear rates at the sliding speed of 1.39 m/s irrespective of base alloy and composites. The difference in wear rates at these two velocities (1.39 m/s and 2.60 m/s) is highest in case of base alloy AZ91, but in case of composites, this difference is decreases as the percentage of reinforcement increases. The wear rate of magnesium alloy and composite is a function of sliding velocity, normal load, and environmental conditions. The variation of wear rate at different velocity and load is due to the presence of different wear mechanism, which is a very complex phenomenon to understand. The observation of wear rate is showing a similar trend is already observed in Chapter 5, that on increasing velocity or load the wear rate is generally increases.

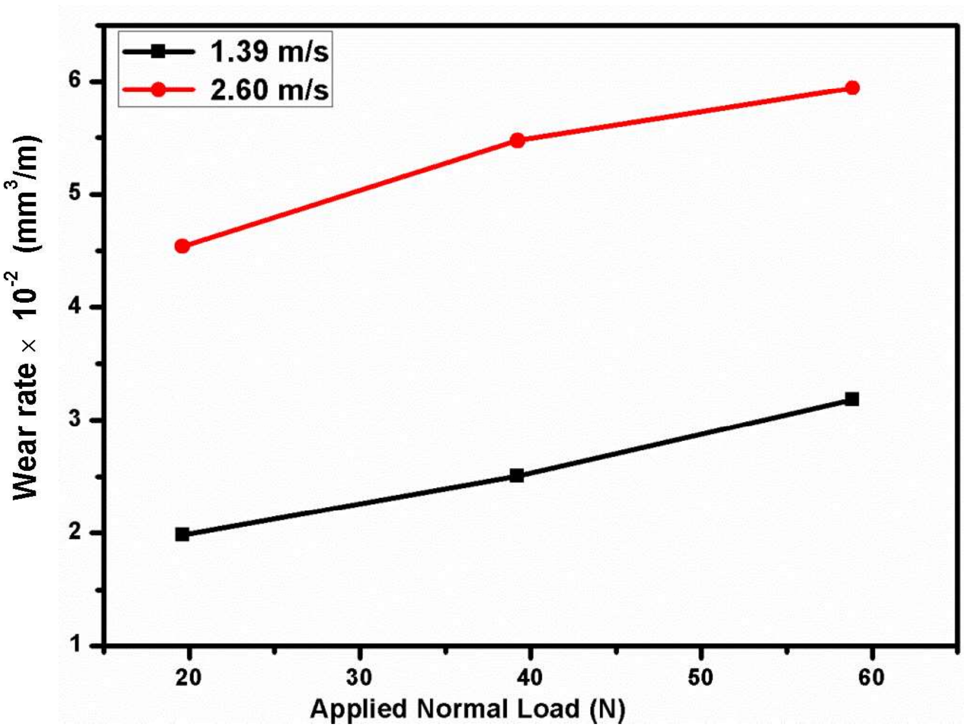

Figure 6. 17: Variation of wear rate of AZ91 magnesium alloy at different velocity and different applied normal load

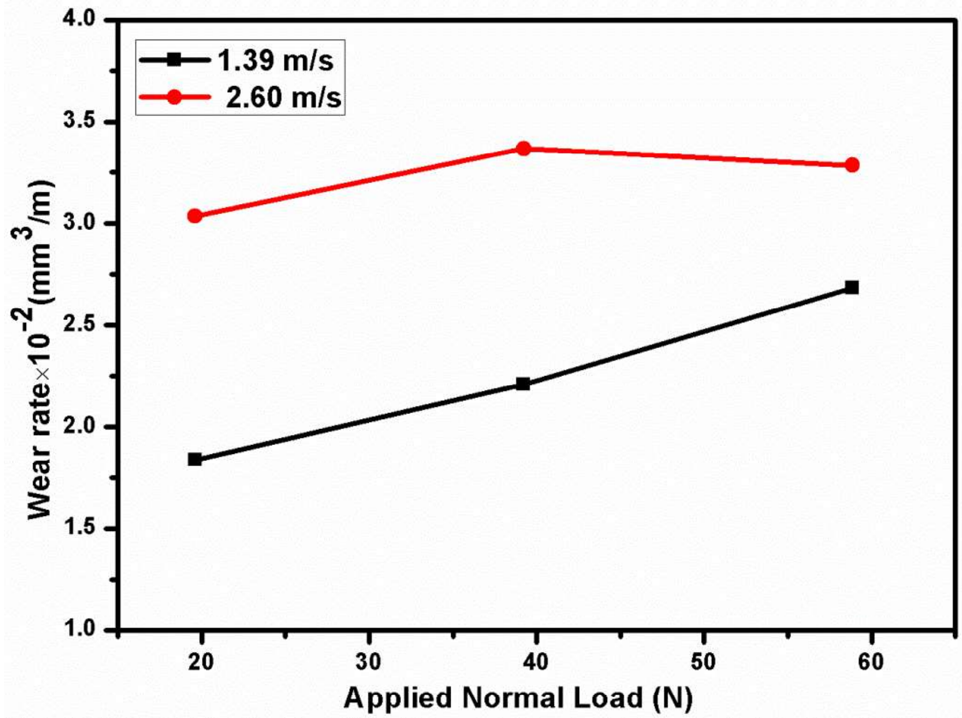

Figure 6. 18: Variation of wear rate of 3 percent weight of TiC in AZ91 magnesium alloy at different velocity and different applied normal load

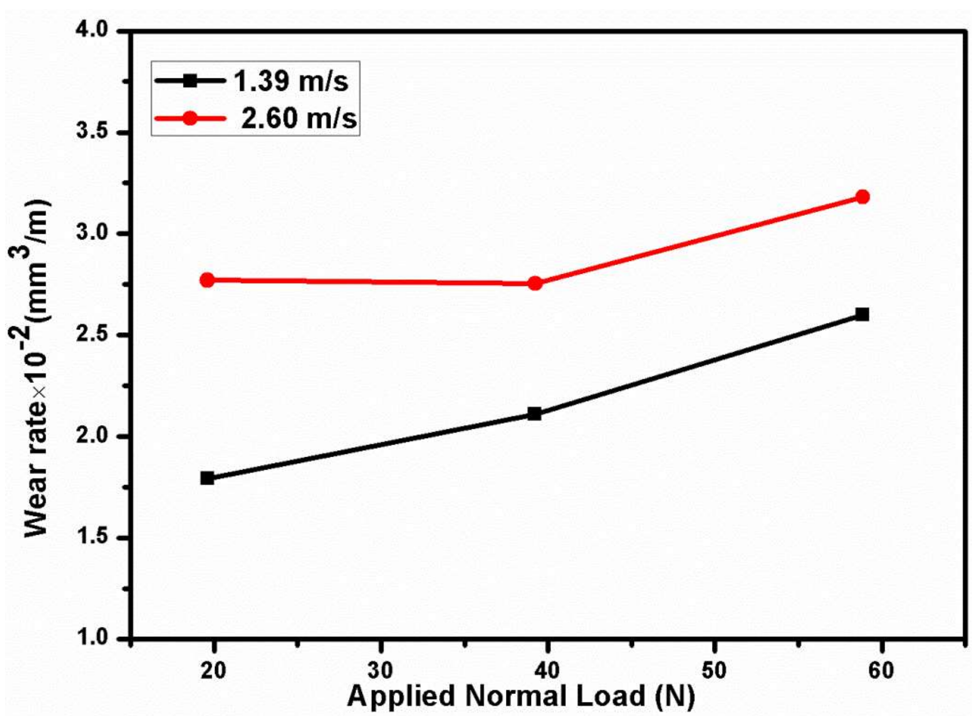

Figure 6. 19: Variation of wear loss of 6 percent weight of TiC in AZ91 magnesium alloy at different velocity and different applied normal load

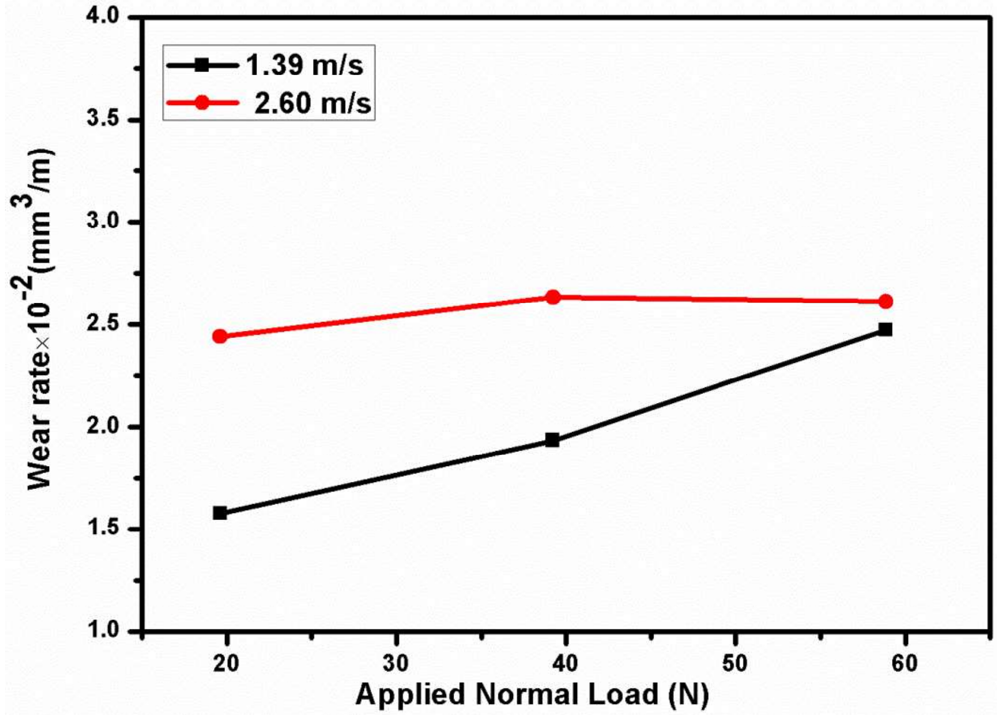

Figure 6. 20: Variation of wear loss of 9 percent weight of TiC in AZ91 magnesium alloy at different velocity and different applied normal load

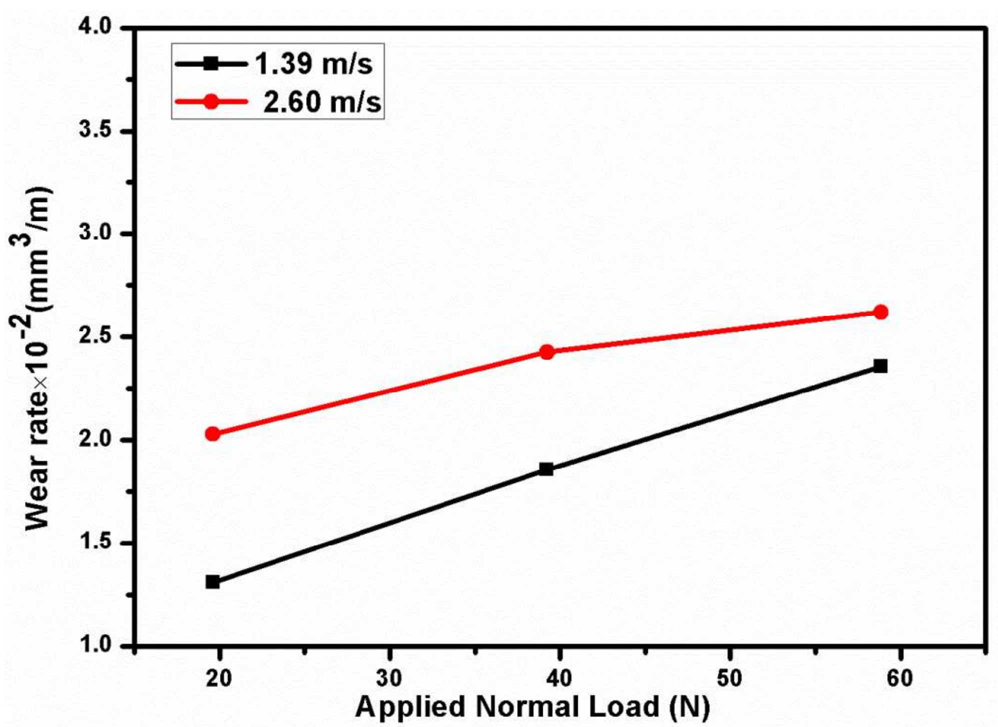

Figure 6. 21: Variation of wear loss of 12 percent weight of TiC in AZ91 magnesium alloy at different velocity and different applied normal load

b) *Examination of sliding surfaces and wear mechanism*

The worn pin surfaces were examined by scanning electron microscope to predict the different wear mechanism occurred during sliding on the hard disk in pin on disk dry sliding wear test. The oxidation wear was observed at low velocity lower normal load. Figure 6.22 shows the selective SEM micrograph of TiC reinforced AZ91 magnesium alloy composites at different load, velocity and weight percentage of reinforcements. In the case of composite plowing delamination and oxidation, wear are prominently present in the worn surfaces. A large amount of accumulated embedded debris is also observed at the worn surfaces of the pin. This behavior is indicative of oxidative wear, which is developed due to frictional and sliding heating of the pin materials. Composite materials exhibit the extensive formation of oxide than unreinforced magnesium alloy. Five different wear mechanism may be operated singly or in combination under different normal load and sliding speed. The wear mechanism may be abrasion, oxidation, delaminating, adhesion and thermal softening and melting. It is very difficult to examine the exact influence of one or others wear mechanism correctly. The wear behavior within this velocity is oxidation at lower load and de-lamination or abrasion wear at higher load. Several grooves and scratch marks parallel to the sliding direction is evidence of abrasion wear. The de-attachment of wear particle occurs in the form of sheet and short cracks roughly perpendicular to the sliding direction. This type of wear mechanism is classified as delamination wear, and it was first introduced by N.P Suh [144]. The oxidation wear also occurred under the test conditions and due to oxidation material surface become dark at the wear surfaces. A summary of different wear mechanism for a different combination of sliding velocity and applied normal load is predicted in Table 6.6. Pins tested at load 19.62 N and 2.6 m/s exhibit series of short cracks nearly perpendicular to the sliding direction. The cracks removed in the form of small broken sheet and flakes is suggested as delamination wear by several researchers [162], [214], [215]. At higher speed 2.60 and higher load 58.86 N the oxidation and delamination are completely converted into adhesion wear. Due to higher load and velocity pin materials become soft; there are also sign of plastic deformation and smearing. The region of the dominance of wear mechanism depends on the normal load and sliding speed. Abrasion, oxidation, and delamination wear mechanism are generally dominant in lower sliding velocity and lower load region while adhesion and thermal softening/ melting are dominant in higher sliding velocity and loads.

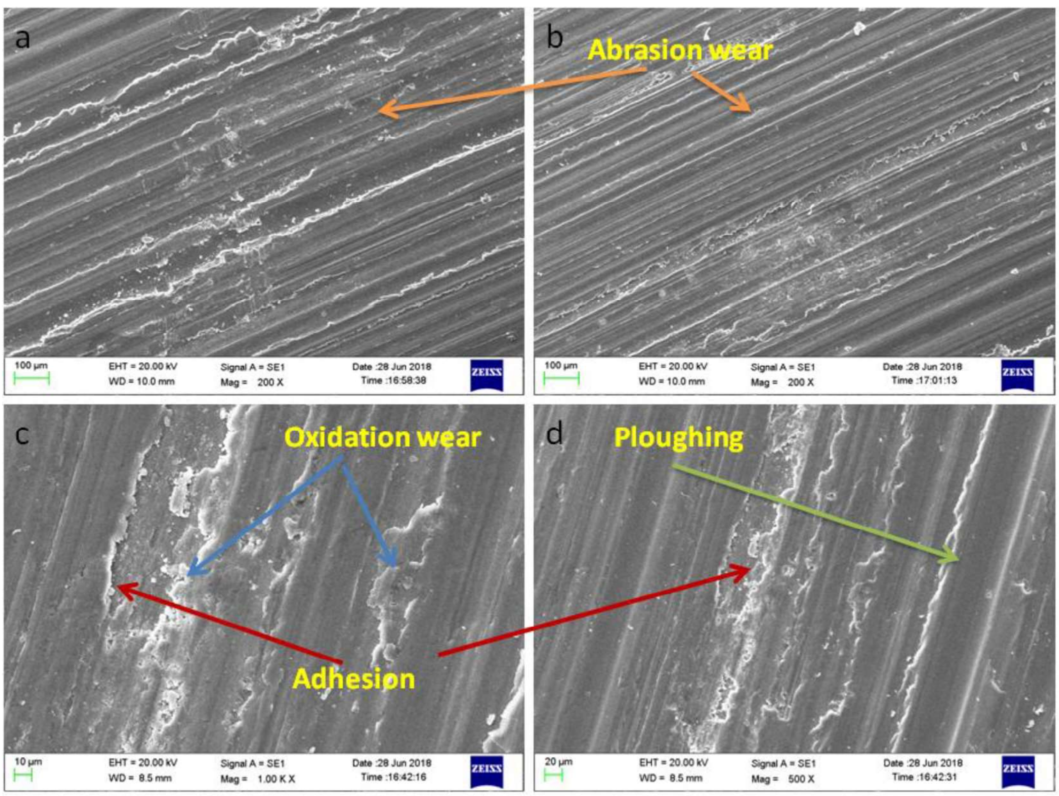

Figure 6. 22: SEM micrographs of the worn surfaces of TiC reinforced AZ91 magnesium alloy composite a) 39.24 N, 1.3 m/s and 6% TiC b) 19.62 N, 2.6 m/s 3% TiC c) 58.86 , 2.6 m/s 9% TiC d) 39.24 N, 2.6 m/s 12% TiC

Table 6. 6: Prediction of wear mechanisms for a different combination of normal load, sliding speed and pin materials

Load (N)	Sliding speed (m/s)	Pin material	Wear Mechanism				
			Abrasion	Oxidation	Delamination	Adhesion	Softening /melting
19.62	1.39	AZ91	*	**	**		
		AZ91+3% TiC	*	**	**		
		AZ91+6% TiC	*	**	**		
		AZ91+9% TiC	*	**	**		
		AZ91+12% TiC	*	**	**		
19.62	2.6	AZ91	*	*	**	*	
		AZ91+3% TiC	*	*	**	*	
		AZ91+6% TiC	*	*	**	*	
		AZ91+9% TiC	*	*	**	*	
		AZ91+12% TiC	*	*	**	*	
39.24	1.39	AZ91	**	**	*	**	
		AZ91+3% TiC	**	**	*	**	
		AZ91+6% TiC	**	**	*	**	
		AZ91+9% TiC	**	**	*	**	
		AZ91+12% TiC	**	**	*	**	
39.24	2.6	AZ91	**	*	*	**	
		AZ91+3% TiC	**	*	*	**	
		AZ91+6% TiC	**	*	*	**	
		AZ91+9% TiC	**	*	*	**	
		AZ91+12% TiC	**	*	*	**	
58.86	1.39	AZ91	*			***	*
		AZ91+3% TiC	*			***	*
		AZ91+6% TiC	*			***	*
		AZ91+9% TiC	*			***	*
		AZ91+12% TiC	*			***	**
58.86	2.6	AZ91	*			***	**
		AZ91+3% TiC	*			***	**
		AZ91+6% TiC	*			***	**
		AZ91+9% TiC	*			***	**
		AZ91+12% TiC	*			***	**

The relative predicted the extent of each wear mechanism: * slight; ** Moderate; *** heavy

The prediction of wear mechanism of TiC reinforced composites for a different combination of normal load, sliding speed and pin materials are almost similar to SiC reinforced because of similar type of particle reinforcement in same matrix material, i.e. AZ91.

6.3. Conclusions

The casting and characterization of TiC particulate reinforced az91 magnesium alloy composites have been performed successfully. The following conclusion that could be drawn from current testing and evaluation:

1. The addition of a small percentage of the hard ceramic particle (TiC_p) is refined the microstructure of the magnesium alloys and form metal matrix composites.
2. The density and porosity of the magnesium alloy composite are increased with an increase in the percentage of TiC particulates.
3. The XRD results peaks are matched with the standard peaks of Mg, and $Mg_{17}Al_{12}$ available in PCPDFwin.
4. The Vickers microhardness value is increased by ~25% on addition of 3% of TiC particulate, and it further increased ~75% on addition of 12 % of TiC particulate.
5. The tensile strength initially decreased and then increased with increase in addition of TiC particulates in magnesium alloys.
6. The Compressive strength is increased by ~2% on addition of 3% of TiC particulate, and it further increased up to ~15% on addition of 12 % of TiC particulate.
7. The composite shows mixed mode fracture (i.e., ductile and cleavage), the fracture surface morphology of the composite also reveals that small size dimple, micro-crack, and cleavage fracture increases with increase in reinforcement.
8. The compression fracture surface of AZ91 exhibit dominant shear failure and showed more shear bands when compared to AZ91 / TiC composites, which on the other hand shows rough fracture surfaces with a mixed mode of shear and brittle features.

9. The wear weight loss and wear rate of the TiC reinforced composites is lower than the unreinforced composites.
10. The average coefficient of friction of the composite is lower than unreinforced alloy, and it is decreased with an increase in normal load.
11. The wear rate at higher sliding velocity is higher, and the effect of the difference in velocity is decreased with an increase in normal loads.